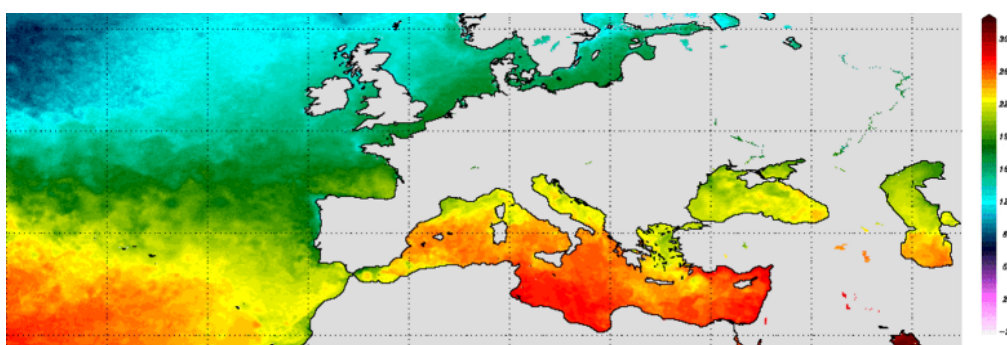# ESA CCI Phase 3 Sea Surface Temperature (SST)

Algorithm Theoretical Basis Document D2.1 v2

Issue Date: **09 January 2021**

ESA REF: ESA/AO/1-9322/18/I-NB

SIGNATURES AND COPYRIGHT

Title   :   **ESA CCI Phase 3 Sea Surface Temperature (SST)**

Volume   :   **Algorithm Theoretical Basis Document D2.1 v1**

Issued   :   **15 December 2019**

Authored :

_____
Prof Chris Merchant (UoR)

Authored :

_____
Dr Owen Embury (UoR)

Address :   University of Reading,
Whiteknights,
Reading,
Berkshire,
RG6 6AH,
United Kingdom

TABLE OF CONTENTS

1.   SCOPE

This is a report in preparation for a comprehensive Algorithm Theoretical Basis Document (ATBD) that will be completed to describe the Sea Surface Temperature Climate Change Initiative Version 3 Climate Data Record (SST CCI v3 CDR). The full ATBD will be document ATBD D2.1 v3.

The form of content of this interim ATBD report is:

- notes in short form elements arising from the algorithm development work between months 9 and 18 within Phase 3 of SST CCI that may be required to be reflected in the full ATBD (D2.1 v3), depending on the final implementation decisions for the v3 CDR

- complete text that may be incorporated in the full ATBD where this has already been prepared in the course of work to date

An further interim ATBD report (D2.1 v1) described algorithm developments achieved during months 1 to 9 of within Phase 3 of SST CCI.

The specific scope of this document is in summary:

- Upgrades to the radiative transfer used for optimal estimation with respect to representation of atmospheric aerosol, exploiting aerosol re-analyses

- Bias-aware optimal estimation (BAOE) theory, and the BAOE tuning results for AVHRRs on NOAAs 8, 9, and 11 (covering the late 1980s)

2. REPRESENTATION OF AEROSOL IN RADIATIVE TRANSFER FOR OPTIMAL ESTIMATION

2.1 Introduction

The Advanced Very High Resolution Radiometers (AVHRRs) are single-view sensors whose retrieval is made using optimal estimation (OE) (see section 0). Part of this retrieval process involves fast radiative transfer simulation, of brightness temperatures and partial derivatives of brightness temperatures with respect to state variables. The climate data record (CDR) from SST CCI in its version 2 ("CDR v2") (Merchant et al. 2019) did not include simulation of tropospheric aerosol within the fast radiative transfer model (RTM) because of limitation of the RTM's capability, and this contributed to the biases present related to desert dust aerosol in particular (Merchant and Embury 2020).

The fast RTM is "RTTOV" , which now has extended capabilities (Saunders et al. 2018). Moreover, more information is available about aerosol distributions from atmospheric re-analyses. This section therefore describes the significant updates to the exploitation of radiative transfer simulation within the SST CCI processing chain.

2.2 The RTTOV model

RTTOV is now available in v12.3, which introduces several improvements over version 11.3 used for CDR v2 including (among others):

- Support for aerosol species used within the Copernicus Atmospheric Monitoring Service (CAMS)

- Support for variable CO_2 concentration

- New solvers for scattering: Discrete Ordinates Method (DOM) and MFASIS

- Optimisation of gas optical depth calculation

- API updates and improvements

In the context of CDR v3 the first two RTTOV updates are the most important. The CAMS aerosol properties allow RTTOV to use the aerosol outputs of the CAMS reanalysis. Variable CO_2 support allows the RTM outputs to include the effect of significant (~30%) changes in atmospheric CO_2 over the last 40 years. In addition, there are now updated gas

transmittance coefficients available for RTTOV 12.3 which make use of the latest spectroscopy and water vapour continuum parameterisation[1].

2.3   RTTOV aerosol coefficients

RTTOV v12.3 is supplied with two sets of aerosol scattering coefficients based on the OPAC and CAMS aerosol types shown in Table 1.

Table 1: OPAC and CAMS aerosol types supported by RTTOV 12.3

OPAC	CAMS
Insoluble	Black Carbon
Water soluble	Dust, bin 1, 0.03-0.55
Soot	Dust, bin 2, 0.55-0.90
Sea salt (acc mode)	Dust, bin 3, 0.90-20.0
Sea salt (coa mode)	Ammonium sulphate
Mineral (nuc mode)	Sea salt, bin 1, 0.03-0.5
Mineral (acc mode)	Sea salt, bin 2, 0.5-5.0
Mineral (coa mode)	Sea salt, bin 3, 5.0-20.0
Mineral transported	Hydrophilic organic matter
Volcanic ash	
New volcanic ash	
Asian dust	

Because temporally evolving tropospheric aerosol estimates are available from the CAMS re-analysis back to 2003, we adopt use of the CAMS aerosol modes (more discussion below).

---

[1] *Details: line-by-line radiative transfer model, LBLRTM 12.8 using "HITRAN2012 spectroscopic coefficients and "MT_CKD" water vapour continuum version 3.2.*

A limitation of the CAMS model is that it does not include a component to represent the stratospheric aerosol from Pinatubo and other volcanic eruptions. Therefore, we have generated additional aerosol scattering properties matching the stratospheric aerosol approach used in CCI Phase 2. These aerosol scattering properties are calculated using Mie theory from input datasets of refractive index and size distribution. We used two sets of data: the "SUSO" refractive index and size distribution from OPAC; and 75% H_2SO_4 at 215 K refractive index data from HIRTAN 2016 (Biermann et al. 2000) size distribution r=0.6, sigma = 1.2. The results are very similar in terms of brightness temperature impact, giving good confidence, although the implied aerosol masses for a given change in brightness temperature do differ significantly.

2.4   Usage of CAMS aerosol information

The CAMS reanalysis (Bozzo et al. 2020) uses ECMWF's 4DVar data assimilation scheme running at spatial resolution of ~80 km (TL255 grid) and 60 vertical model levels (from 0.1 hPa to surface), the analyses time-step is 3 hours. However, the CAMS reanalysis period is 2003 to 2018 so it does not cover the full period of the SST-CCI processing. In order to process the full SST-CCI period and reduce the required data download to a manageable volume we use the CAMS aerosol climatology (Bozzo et al. 2020); this provides us with profiles of aerosol loading for a given month and location.

To represented interannual variability of aerosol within the SST CCI processing, the profiles from the climatology are scaled to match time-specific column aerosol mass loadings when available. In other words, interannual variability in amount of aerosol can be accommodated, but the relative vertical distributions are always climatological.

The CAMS aerosol climatology provides monthly layer-integrated mass concentrations (kg/m^2) for 11 aerosol components on 60 model levels and 3° × 3° horizontal grid. The components are: Sea Salt bin1 (0.03-0.5 μm); Sea Salt bin2 (0.5-5.0 μm); Sea Salt bin3 (5.0-20.0 μm); Mineral Dust bin1 (0.03-0.55 μm); Mineral Dust bin2 (0.55-0.9 μm); Mineral Dust bin3 (0.9-20.0 μm); Organic Matter (hydrophilic); Organic Matter (hydrophobic); Black Carbon (hydrophilic); Black Carbon (hydrophobic); (tropospheric) Sulfates.

We undertook simulations of aerosol impact on brightness temperatures for typical SST sensors to understand the relative importance of these types. Mineral dust aerosols were, as expected, the most impactful, with impacts of order 1 K (for affected locations). All other types affect brightness temperature at levels mostly <0.1 K, but over larger portions of the world. Since the impact of several modes could reach of order 0.1 K, this remains relevant to SST, although not large, and so we decided to include all aerosol types in the simulations to simulate relevant impacts whenever present.

The RTTOV simulations influence both cloud detection and the OE. Simulations are performed on the full state vector, which is supplied by weather re-analysis profiles (next section) and all the CAMS aerosol types as noted previously.

There are two ways in which aerosols can be implemented, according to whether we treat the aerosol information as a fixed parameter of the simulations, or as a parameter which may be estimated. Fixed parameters are included in the full state vector for simulation, but do not appear in the reduced state vector of parameters that may be retrieved. This approach is used for all the parameters other than mineral dust. The mineral dust profiles are also included in the full state vector for simulation, and additionally the total dust mass (integrated vertically and with respect to particle size) is included in the reduced state vector, which means it may be retrieved. Where a sensor has insufficient spectral information to be informative about dust, including for AVHRRs, the dust mass is nonetheless not retrieved, but the availability to the reduced state vector enables retrieval from other sensors with more channels, which will be of relevance in future work (towards CDR v4).

The sequence of use of the CAMS aerosol information in L1 processing is as follows:

1. Load Climatology

2. Interpolate to required latitude/longitude/time using tri-linear interpolation (treating each 12 monthly mean as the instantaneous value at the 15th day of each month)

3. Use surface pressure to calculate sigma pressure levels and interpolate to NWP pressure levels (interpolation linear in log pressure)

4. Convert from cumulative mass to layer mass

5. Convert to mass mixing ratio (kg/kg)

   o layer aerosol (kg/m^2) / layer thickness (km) = aerosol density (g/m^3)

   o aerosol density (g/m^3) / air density (g/m^3) = mass mixing ratio (kg/kg)

   o NOTE – RTTOV requires mmr with respect to moist air so air density is calculated for dry-air + water vapour

6. If total column aerosol quantities are available (i.e., for 2003 to 2018, presently from the CAMS re-analyses column-mass data), scale climatological profiles to match the given total column mass.

7. Use (scaled) profiles in the RTTOV simulation.

The RTTOV simulations are first used within Bayesian cloud detection, and then within OE (for AVHRRs).

2.5   Weather re-analysis data: ERA-5

The European Centre for Medium-range Weather Forecasting re-analysis 5 (ERA-5) (Hersbach et al. 2018) is at higher resolution and maintained beyond the cut-off date in 2019 of the previously used re-analysis (ERA-Interim). It is therefore used within SST CCI. In conjunction with the RTTOV developments coded within the CCI processor as described above, support for ERA-5 atmospheric data has been implemented.

Unfortunately, at the time of initiating processing for CDR v3, the data store used for SST CCI processing has accumulated ERA-5 data covering 2000 onwards, not the full record. It has been decided therefore to use ERA-5 for Metop AVHRRs. NOAA AVHRRs (used within SST CCI until both Metop-B and SLSTR-A are available) will, for their mutual consistency, be processed using ERA-Interim in CDR v3.

Use of ERA-5 should have a positive impact and exclusively using it would be preferable, but the impact on the CDR v3 should be small, since the parameterisation of the OE retrievals (see next section) is undertaken using the same dataset, ERA-Interim for NOAA AVHRRs, as used in L1 processing.

3. BIAS-AWARE OPTIMAL ESTIMATION (LATE 1980S)

3.1 Sea surface temperature retrieval

Optimal estimation (OE) is a widely used inverse method in geophysics and remote sensing (Rodgers 2000). OE has been applied to retrieval of sea surface temperature from space-based imagery (Kilic et al. 2018; Merchant et al. 2008; Merchant et al. 2009) as well as for many problems in atmospheric sounding (Carboni et al. 2019; McGarragh et al. 2018; Poulsen et al. 2012; Thomas et al. 2009). The most common formulation for SST retrieval jointly estimates the radiometric skin temperature, x, and the total column water vapour (TCWV), w. This is a reduced state vector, $z = [x, w]^T$, since the clear-sky brightness temperatures observed by the satellite, y, depend in general on a much longer list of state variables, x, including the vertical distribution of atmospheric temperature and humidity, the sea state and atmospheric aerosols.

OE requires a physical model of the observations, which in this case means a radiative transfer model (RTM) that operates on the full state vector, $F(x_a)$. The subscript a here indicates *a priori*, meaning that the RTM is run on the prior estimate of the surface temperature and atmospheric state before retrieval. The prior state generally is obtained from a numerical weather prediction forecast or analysis. The physical model is also differentiated with respect to the retrieved variables:

$$K = \frac{\partial F}{\partial z}$$

Eq. 1

The retrieved state, $\hat{z}$, corresponds to the prior state, z_a, modified by the difference between the satellite observations and the expected brightness temperatures as simulated by the RTM on the prior state. This difference is transformed from the observation space to the state space by a gain matrix that accounts for the sensitivity of the brightness temperatures to the state variables Eq. 1 and the relative uncertainty of the observations and prior state:

$$\hat{z} = z_a + (K^T S_\epsilon^{-1} K + S_a^{-1})^{-1} K^T S_\epsilon^{-1}(y - F)$$

Eq. 2

Here, S_ϵ characterises the error distribution in the observations relative to the simulations as an error covariance matrix. The uncertainty in each brightness temperature is given by the square root of the diagonal values of this matrix, while the off-diagonals indicate the strength of covariance (and, thus, correlation) of those errors. Similarly, the error covariance matrix of the prior information is S_a, whose first diagonal term is the square of the uncertainty in the prior estimate of SST. If the error distributions of z_a and $y - F$ are zero-mean, the retrieved value will have zero mean expectation of error. If the error

9

distributions are gaussian and correctly characterised by S_ϵ and S_a, the retrieved values will be an optimal solution and their uncertainty will be accurately characterised by the retrieval error covariance matrix $S = (K^\mathrm{T} S_\epsilon^{-1} K + S_a^{-1})^{-1}$, which may be calculated as part of the evaluation of Eq. 2.

To obtain optimal estimates, therefore, the prior must be unbiased, the satellite calibration and radiative transfer simulations need to be negligibly biased with respect to each other and good estimates of two error covariance matrices need to be available. To meet these conditions for a system of n_y observations and n_z retrieved variables, we need good estimates of the following: $n_y + n_z$ bias correction parameters (more if there are systematic tendencies which are fitted rather than a single offset); $n_y + n_z$ uncertainty estimates (which again may vary according to the circumstances of the retrieval); and $\frac{1}{2} n_y (n_y + 1) + \frac{1}{2} n_z (n_z + 1)$ error correlation coefficients. For even the minimal system of retrieving SST and TCWV using three infrared brightness temperatures, this corresponds to 14 retrieval parameters if no parameter dependency is fitted. Some relevant information to constrain these parameters is generally available, such as error correlation being zero between independent sources of information, or estimates of instrument noise from sensor specifications or the onboard calibration system. Nonetheless, in past implementations, e.g. Merchant et al. (2009), simplifications such as diagonal error covariance matrices (Rodgers 2000) have been used along with judgements about many parameters. This element of judgement has been strongly criticized (Koner and Harris 2016; Koner et al. 2015) and alternative inverse methods have been proposed with fewer parameters. The alternative response, pursued here, is to exploit a means of systematically evaluating the retrieval parameters, to which we refer as "bias-aware" optimal estimation.

3.2   Bias parameter estimation

Bias-aware optimal estimation (BAOE) combines the following elements: the insight in Rodgers (2000) that uncertain retrieval parameters can themselves be retrieved across a large number of retrieval instances; the idea that anchoring the system to some reference data that are taken to be unbiased can help disambiguate biases arising from different sources; and the use of expressions derived as diagnostics in data assimilation (Desroziers et al. 2005) as means of objectively estimating error covariances (Cordoba et al. 2017; Waller et al. 2016) after bias-correction. Merchant et al. (2020) (hereafter M20) presented a BAOE approach with reference to in situ references, and in Merchant et al. (2020) an approach for cross-satellite harmonisation of sea surface temperature is demonstrated. In this paper, in situ references are again used, but the derivation of the bias parameters is reformulated (relative to M20) to reduce complexity and the amount of radiative transfer modelling involved.

Observational biases are generally present, and mean that errors $y - F$ do not have zero mean over a large ensemble of retrievals. The retrieved value is sensitive to the bias in this difference, irrespective of whether the source of bias is in the satellite calibration or in the forward model. We formulate the bias parameters, β, as corrections to be added to the forward model, but this choice does not imply that the forward model is the only or main source of systematic errors.

The prior estimate of the state may also have non-zero mean error across many instances of retrieval. Previous results (M20) suggest that clear-sky areas of infrared imagery have lower TCWV than prior NWP humidity profiles; since these are all-sky profiles, this is physically plausible. Corrections for prior bias, γ, are defined such that $z_a + \gamma$ will be unbiased.

The β and γ parameters are included in the extended state (retrieved) vector, $\tilde{z}$. To anchor the estimate of observational biases, reference data (see §**Error! Reference source not found.**) are included as additional observations in the observation vector, $\tilde{y}$. (This is the point of difference between the approach here and M20. In M20, the forward model was run using the reference data for the SST, rather than using the usual prior SST source for the retrieval as here. This is a simplification in procedure, since simulations for the latter source are naturally available from the satellite data processing chain.)

The error covariance matrices are initially specified using expert knowledge and any information available on error sources such as instrument noise. The bias-correction parameters will be best estimated if the error covariances matrices are well estimated. Conversely, the error covariance matrices need to characterise the uncertainties after bias corrections have been applied. The iterative update of the error covariance matrices is therefore necessary and is discussed in §3.3.

Using the initial estimates of error covariance matrices, the extended optimal estimator is solved across a large sample of cases for which in situ reference data are available. These cases are hereafter referred to as 'matches' since matching of the satellite data and in situ data is required, as described in §**Error! Reference source not found.**. The matches are randomised, to ensure independence of consecutive iterations with respect to geophysical parameters and errors in individual reference values. Updated bias parameters (and their uncertainties) are passed between iterations. The equation for the ith iteration thus uses the bias parameters retrieved in the $i - 1^{th}$ retrieval. For the case where the reference data are measured values of SST, x_r having estimated uncertainty u_r, and the bias in the prior TCWV, γ, is to be estimated, the extended OE equation is:

$$\tilde{z}_i = \tilde{z}_a + \left(\widetilde{K}^{\mathrm{T}}\tilde{S}_\epsilon^{-1}\widetilde{K} + \tilde{S}^{-1}\right)^{-1}\widetilde{K}^{\mathrm{T}}\tilde{S}_\epsilon^{-1}\left(\tilde{y} - \left(\widetilde{F}(\tilde{z}_a) + \gamma_{i-1}\,\partial\widetilde{F}/\partial w + \widetilde{\beta}_{i-1}\right)\right)$$

$$\tilde{z}_a = \begin{bmatrix} x_a \\ w_a + \gamma_{i-1} \\ \gamma_{i-1} \\ \beta_{i-1} \end{bmatrix}$$

$$\tilde{y} = \begin{bmatrix} y \\ x_r \end{bmatrix}$$

$$\widetilde{F}(\tilde{z}_a) = \begin{bmatrix} F(z_a) \\ x_a \end{bmatrix}$$

$$\widetilde{\beta}_{i-1} = \begin{bmatrix} \beta_{i-1} \\ 0 \end{bmatrix}$$

Eq. 3

$$\widetilde{K} = \begin{bmatrix} \partial F/\partial x & \partial F/\partial w & \partial F/\partial w & I \\ 1 & 0 & 0 & 0 \end{bmatrix}$$

$$\tilde{S} = \begin{bmatrix} S_a + \begin{bmatrix} 0 & 0 \\ 0 & u_{\gamma_{i-1}}^2 \end{bmatrix} & 0 & 0 \\ 0 & u_{\gamma_{i-1}}^2 & 0 \\ 0 & 0 & S_{\beta_{i-1}} \end{bmatrix}$$

$$\tilde{S}_\epsilon = \begin{bmatrix} S_\epsilon & 0 \\ 0 & u_r^2 \end{bmatrix}$$

$$\tilde{z}_i = \begin{bmatrix} \hat{x}_i \\ \hat{w}_i \\ \gamma_i \\ \beta_i \end{bmatrix}$$

The form of this extended retrieval is identical to Eq. 1., and Eq. 3 is written explicitly to show how extension of the state and observation vectors leads to extended forward model, partial derivative and error covariance matrices. After the retrieval of the extended state vector for the ith match, the updated parameters are passed to the next randomly selected match, and the parameters are thus progressively updated. The principle is analogous to model parameter estimation using Kalman filtering (Kalman 1960) but without any concept of continuity in time. Graphs of the evolution of the iterative β and γ parameter estimates are inspected to ensure convergence, and $O(10^5)$ iterations are required for a given pass.

Eq. 3 is written as if β and γ are constants for a given bias-corrected quantity. This would not be adequate representation of the systematic dependencies observed. For example, the correction of a given brightness temperature may need to depend on factors such as satellite zenith angle, slant path integrated water vapour and/or instrumental parameters,

for example. Context-dependent corrections are estimated by deriving different parameter values from only those matches falling within sub-ranges of auxiliary quantities, and using these values to define a piecewise linear correction function.

For example, the correction of the prior total column water vapour, w_a, has been derived as a function of its own uncorrected value. The range of w_a in matched data typically ranges from close to zero (dry, high-latitude locations) to ~60 kg m^{-2} (regions of convergence in the tropics). This range is split into n_γ sub-ranges (hereafter, "bins", index $j \in \{1 \dots n_\gamma\}$). In a given iteration, i, of Eq. 3, the prior water vapour is interrogated to identify the value, J, of j (i.e., in which bin w_a lies). γ actually comprises n_γ parameter values, γ_j, one for each bin, and the iteration i updates $\gamma_{j=J}$, while the parameter values $\gamma_{j \neq J}$ are not modified. The mean prior water vapour in each bin, $\overline{w}_j$ is also calculated. The full γ correction is defined as the piecewise linear interpolation with respect to w_a between the (final iterated) values $\gamma(\overline{w}_j) = \gamma_j$. Extrapolation is not used, and for $w_a < \overline{w}_1$ the correction is fixed at $\gamma(w_a) = \gamma_1$, and similarly for $w_a > \overline{w}_{n_\gamma}$ the correction is fixed at $\gamma(w_a) = \gamma_{n_\gamma}$.

Piecewise linear correction is also used for the adjustment of brightness temperature for each infrared channel in use. To obtain a correction that accounts for more than one dependency, cumulative piecewise linear corrections are calculated. If the n_q auxiliary quantities for the brightness temperature corrections (e.g., satellite zenith angle, etc) are $q_k : k \in \{1 \dots n_q\}$ and $L_{c,k}(q_k)$ is the piecewise linear function defined by interpolated between the derived parameter values $\beta_{c,k}(\overline{q}_{k,j})$, then the total brightness temperature correction is

$$\beta_c \left(q_1, \dots, q_{n_q} \right) = \sum_{k=1}^{n_q} L_{c,k} \qquad \text{Eq. 4}$$

for the given channel, c. The choice of auxiliary quantities could in principle differ between channels according to insights into any channel-specific problems, but in the present implementation the same auxiliary quantities are used for all infrared channels of a given sensor.

To obtain $\boldsymbol{\beta}$ values that add cumulatively (Eq. 4), they are derived sequentially. Correction parameters $\beta_{c,1}(\overline{q}_{1,j})$ with respect to auxiliary quantity q_1 are obtained by iterative application of Eq. 3 with no other corrections applied. Then, applying the corresponding correction $L_{c,1}(q_1)$ to $\boldsymbol{F}$ for each iteration i, the iterative procedure is applied again for the auxiliary quantity q_2, and so on.

3.3   Covariance matrix estimation

The estimation of the bias correction parameters described in the previous section is initially done using observation and prior error covariance matrices, S_ϵ and S_a, that are obtained by experience, expert judgement and information such as sensor noise estimates (from the literature or from the onboard calibration processes). It has been noted even in the earliest implementations of OE for SST retrieval (Merchant et al. 2008) that it would be preferable to have more objective means of determination, and BAOE provides this by adapting expressions originally brought together in Desroziers et al. (2005).

The observation error covariance (which accounts for uncertainty in satellite calibration, noise and radiative transfer simulation) is first re-estimated after the bias corrections for the brightness temperatures are applied. The first step is to undertake joint retrieval, $\hat{z}$, of the state using the extended observation vector (corrected brightness temperatures and the reference data) across the full set of matches. The statistics of the result are then used to update S_ϵ using:

$$\widehat{\widehat{S}}_\epsilon = \begin{bmatrix} \widehat{S}_\epsilon & D \\ D^{\mathrm{T}} & \hat{u}_r^2 \end{bmatrix} = \frac{1}{2}\langle d_r^o d_a^{o\,\mathrm{T}} + d_a^o d_r^{o\,\mathrm{T}} \rangle$$

$$d_r^o = \widetilde{y} - \widetilde{F}(\hat{z}) - \langle \widetilde{y} - \widetilde{F}(\hat{z}) \rangle$$

Eq. 5

$$d_a^o = \widetilde{y} - (\widetilde{F}(\hat{z}) - \widetilde{K}_{\hat{z}}(\hat{z} - z_a)) - \langle \widetilde{y} - (\widetilde{F}(\hat{z}) - \widetilde{K}_{\hat{z}}(\hat{z} - z_a)) \rangle$$

Eq. 5 is formulated explicitly to show use of de-meaned residuals and how to make the estimated matrix symmetric. $\widehat{S}_\epsilon$ provides improved observation uncertainty information on its diagonal, and information about error correlations via the off-diagonal terms. Satellite noise is not expected to be correlated between channels, although there are exceptions, e.g., Holl et al. (2019). However, calibration and simulation errors may involve cross-channel correlations, which previously have been poorly known. This also provides an updated estimate, $\hat{u}_r$ for the reference data uncertainty, which is useful since it is not necessarily well quantified up front, particularly further back in time.

Instrumental uncertainty expressed as noise in brightness temperatures are typically scene dependent, because of non-linearity of the radiance-temperature relationship (which is the channel-integrated Planck function). The component of "observation error" that comes from the radiative transfer simulation is expected to be variable: the approximations of fast radiative transfer simulations are more uncertain when the optical path length from surface to sensor increases. It is reasonable, therefore, to estimate S_ϵ as a piecewise linear function of a quantity that correlates somewhat with both brightness temperature and optical path

length of a quantity that correlates usefully with brightness temperature and infrared optical path length. We use the slant-path integrated water vapour (hereafter "WV path") for this purpose (i.e., $w\sec(\theta)$, where θ is the satellite zenith angle). Eq. 5 is applied to subsets of the matches falling within bins of WV path to obtain the piecewise linear dependence.

Having obtained an improved estimate of S_ϵ the next step is to update the prior error covariance, S_a. For this, a new set of SST retrievals is made, now incorporating the new estimates of the observation error covariance as well as the brightness temperature corrections. The differences of the retrieved and prior state are used to estimate S_a.

The diagonal of S_a contains the squares of the uncertainty in prior SST and prior TCWV. The uncertainty in each depends on the source of prior information, is likely to increase for earlier times and may be geographically variable. The possibility of time-dependence is incorporated in our implementation only indirectly by estimating S_a separately for different sensors. To capture to some degree the possibility of large-scale variations in these uncertainties, S_ϵ is estimated for bins of prior SST itself, which varies with latitude and correlates with TCWV. This is done by applying Eq. 6 to matches falling within sub-ranges of the SST distribution.

$$\widehat{S}_a = \frac{1}{2}\langle (K^\mathrm{T}K)^{-1}K^\mathrm{T}\left(d_a^r d_a^{o\,\mathrm{T}} + d_a^o d_a^{r\,\mathrm{T}}\right)K(K^\mathrm{T}K)^{-1}\rangle$$

Eq. 6

$$d_a^r = K(\hat{z} - z_a) - \langle K(\hat{z} - z_a)\rangle$$

We also have strong expectations for S_a. The value of the prior SST uncertainty should, when combined in quadrature with the reference SST uncertainty, correspond closely to the standard deviation between the prior and the reference. In our implementation, we constrain this to be the case. The off-diagonals should be zero, since we do not expect error correlation between SST and TCWV, and in our implementation the implied correlation coefficients are inspected to verify they are small (they are generally <0.25 in magnitude) and then set to zero. In contrast, the TCWV uncertainty embodied in the estimate of S_a is not otherwise well quantified and is used unmodified thereafter.

Some practical measures to stabilize the calculation of Eq. 5 and Eq. 6 are implemented. In evaluating $\langle d_r^o d_a^{o\,\mathrm{T}} + d_a^o d_r^{o\,\mathrm{T}}\rangle$, a trimmed mean is used to avoid undue influence of a small fraction of outliers. $K^\mathrm{T}K$ is inverted in Eq. 6, and is occasionally (typically for <0.5% of matches) ill-conditioned. In our implementation, matches for which the condition number of $K^\mathrm{T}K$ exceeds 10^6 are excluded from the evaluation.

Commercial in Confidence

ESA/AO/1-9322/18/I-NB · · · · · · · · · · ESA CCI Phase 3 Sea Surface Temperature (SST) · · · · · · · · · · 9 January 2021

Algorithm Theoretical Basis Document D2.1 v2

3.4   Other aspects of implementation

As described in (Merchant et al. 2020), the sequence of bias correction and updating covariance matrices is cycle through iteratively (two complete cycles followed by the final bias correction step). This is needed so that the bias corrections and covariance parameters have the opportunity to respond to each other during optimization.

The process is coded semi-automatically. Expert intervention arises in terms of choosing the auxiliary quantities used for each sensor. This is based upon inspection of the patterns of residual biases seen in untuned EO results obtained before the BAOE process.

3.5   Preliminary results

Results for bias correction parameters are presented here for NOAA 8, 9 and 11. Since results for covariance matrices are directly relevant to uncertainty evaluation of retrievals, these are documented in the end-to-end uncertainty characterisation report (E3UB) v2.

These results are preliminary because the change in covariance matrices will also modify (should improve) the performance of cloud detection. This may require a further cycle of parameterisation to reveal the full benefit (this is to be determined).

3.5.1   Impact of parameterising OE

Before the BAOE cycle of parameterisation was run, the "out-of-the-box" performance of OE is assessed on quality level 5 drifting-buoy-AVHRR matches from the SST CCI matchup data system (Block et al. 2018). This OE uses the fast radiative transfer including (for these sensors) climatological aerosol as described in section 2. In that sense the "untuned" OE is already an improvement on the CDR v2 OE (although "external" SST correction algorithms used in CDR v2 are omitted). The before-and-after results are shown in Table 2. The NOAA 8 and 9 results apply for their respective mission lifetimes and the NOAA 11 results to the years 1988 to 1990 inclusive. (For sensors that last more than 3 years, BAOE will be applied to subsets of the mission lifetime.)

It is notable how few matches there are with NOAA 8 AVHRR. This AVHRR has only night-time observations, since its thermal channels comprise only the 3.7 and 11 um channels. There were also relatively fewer drifting buoys at any given time during its mission. We have not used NOAA 8 in CDR v2, and the decision for CDR v3 requires further analysis.

The NOAA 9 and NOAA 11 results represented the combined statistics for day and night matches. Even untuned, these sensors' biases overall are more or less within the target (0.1 K), although it should be noted that the retrievals are started from a debiassed prior,

Commercial in Confidence

ESA/AO/1-9322/18/I-NB   ESA CCI Phase 3 Sea Surface Temperature (SST)   9 January 2021
Algorithm Theoretical Basis Document D2.1 v2

which helps this to be the case. Nonetheless, the biases are improved overall. More important than the modest bias improvements, however, is the lack of statistically important systematic variations in bias that is achieved, shown in some illustrative plots for NOAA 11 in Figure 1.

Table 2: Summary effect of bias aware parameterisation

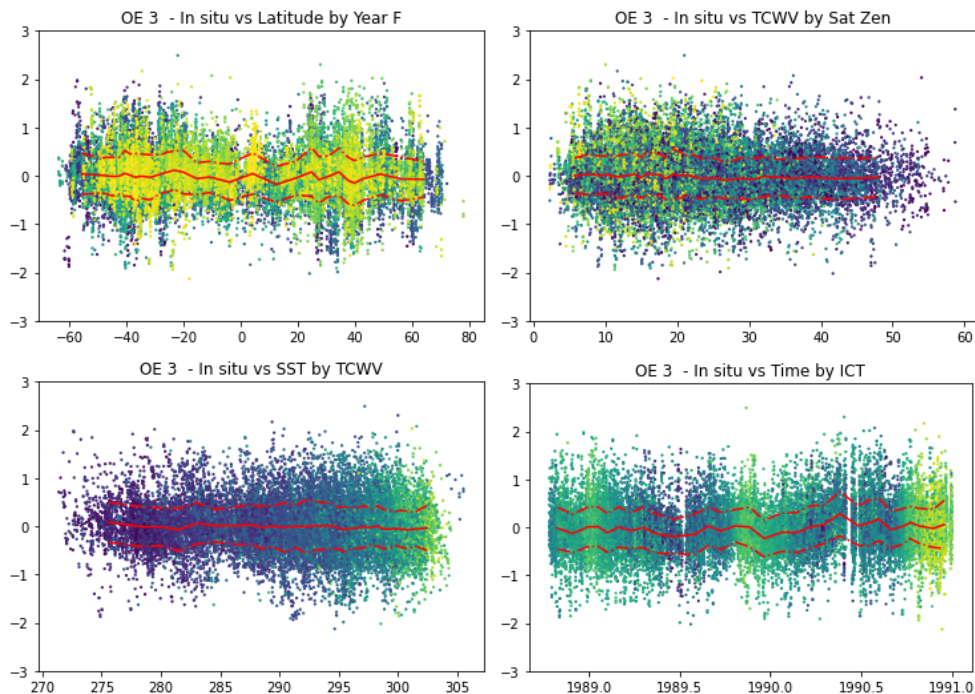| Sensor	N	Untuned OE / cK				Bias-aware OE / cK			
		Mean	Standard deviation	Median	Robust SD	Mean	Standard deviation	Median	Robust SD
N 08	876	15	65	**16**	**64**	0	58	**0**	**55**
N 09	48088	9	64	**13**	**54**	0	61	**5**	**50**
N 11	45275	6	50	**6**	**44**	0	49	**0**	**42**

Figure 1: Example dependence plots for NOAA 11 after BAOE. Vertical axes are all satellite-reference differences in kelvin. Solid lines show binned means of the data, and dashed lines their standard deviation. Points are additionally coloured by a further variable. Top left: differences against latitude. Top right: differences against TCWV. Lower left: differences against prior SST. Lower right, differences against time as year fraction.

17

3.5.2   Brightness temperature bias corrections

The **β** parameters for each sensor are defined against up to four auxiliary quantities, which may differ between sensors. For example, some sensors (e.g. NOAA 8) exhibit strong bias across track in the untuned data (as an asymmetric function of element number) whereas tuning with respect to element is not needed for every case.

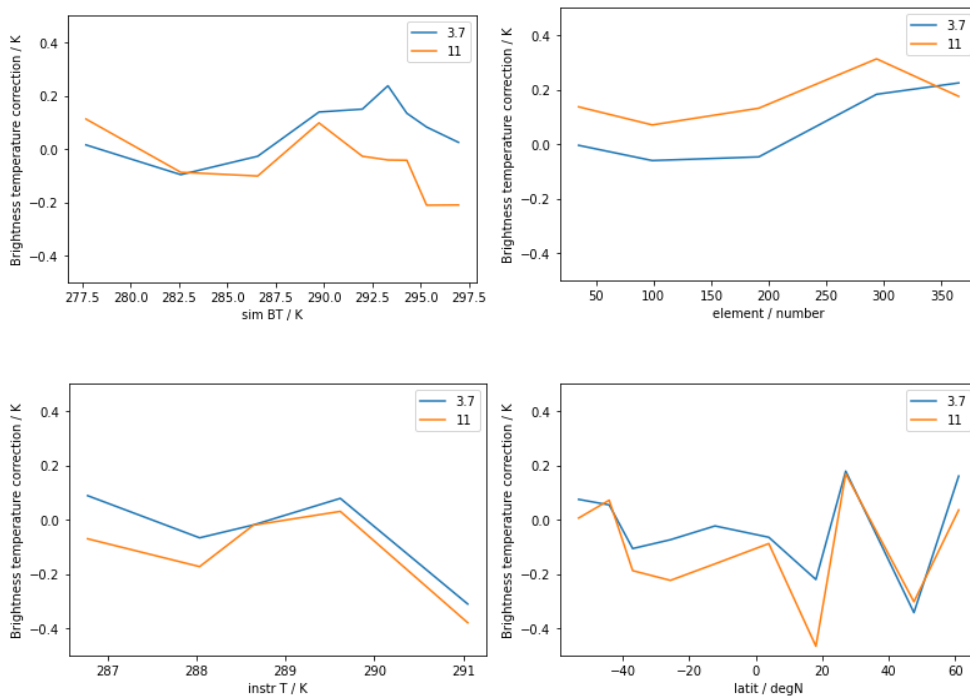The bias correction results are shown in the following figures.

Figure 2. Brightness temperature correction coefficients for NOAA 8. These are piecewise linear functions against (top left) the simulated prior brightness temperature, (top right) the across-track element, (lower left) the instrument temperature and (lower right) latitude.
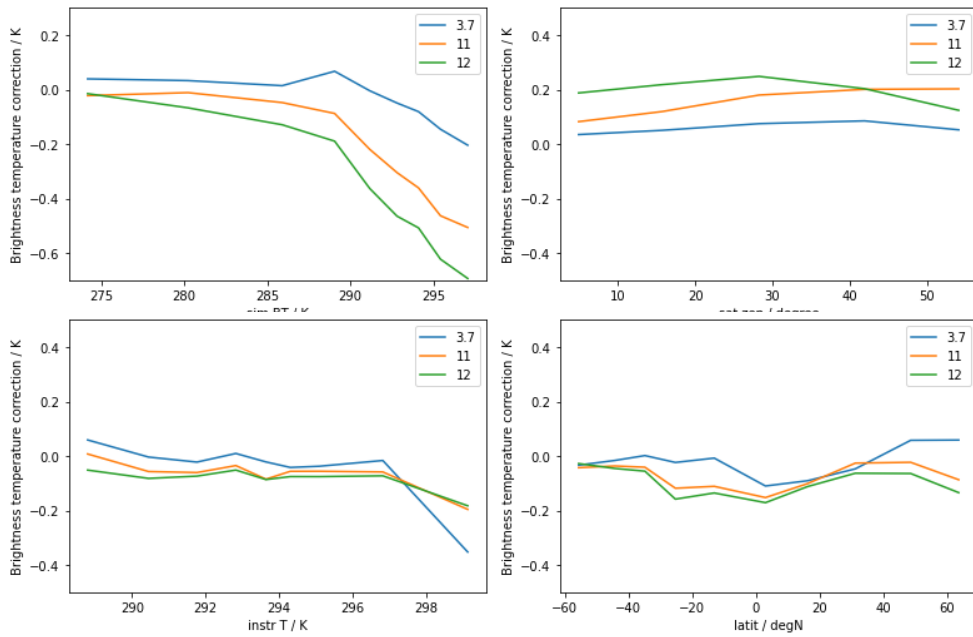
Figure 3. As Figure 2 but for NOAA 9 against the following respective auxiliary quantities: simulated brightness temperature, satellite zenith angle, instrument temperature, latitude.
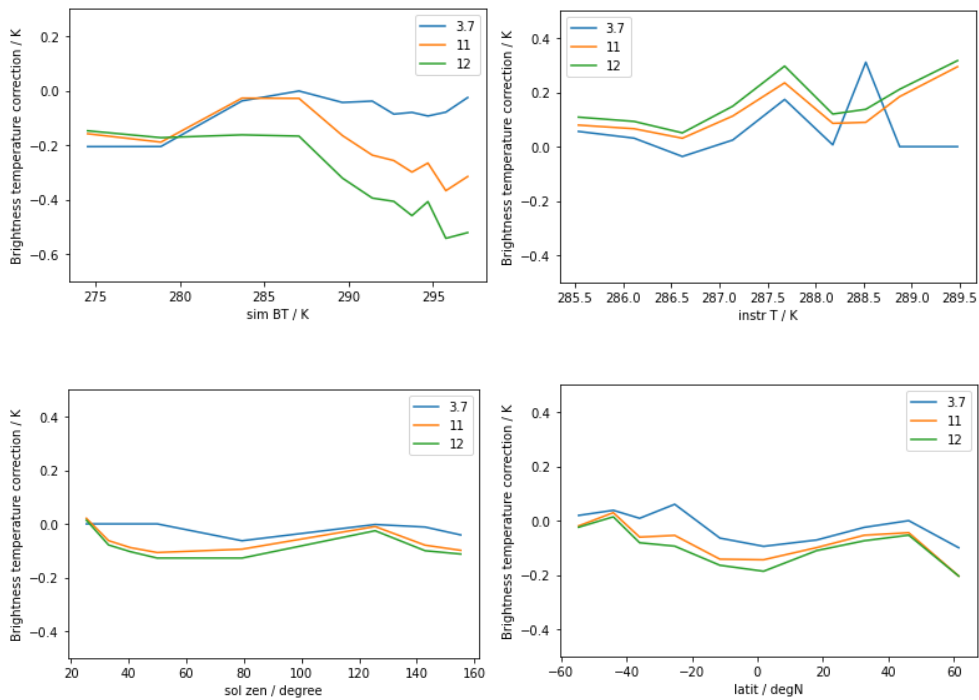

Figure 4. As Figure 2 but for NOAA 9 against the following respective auxiliary quantities: simulated brightness temperature, instrument temperature, solar zenith, latitude.

19

Commercial in Confidence

ESA/AO/1-9322/18/I-NB   ESA CCI Phase 3 Sea Surface Temperature (SST)   9 January 2021
Algorithm Theoretical Basis Document D2.1 v2

It is notable that all the channels in a given sensor tend to behave similarly in terms of functional variation. This could arise either because of calibration effects or simulation effects that tend to be in common with respect to the various auxiliary quantities.

3.5.3   Water vapour correction

The TCWV from re-analysis represents the all-sky quantity, whereas for IR SST retrieval we are considering only clear-sky areas, where humidity is below saturation level unlike in clouds. Therefore, it is reasonable to expect that the TCWV is overestimated for our application. It is therefore of interest that for all the sensors, the estimated TCWV correction dependence is such that the TCWV is corrected to lower values.
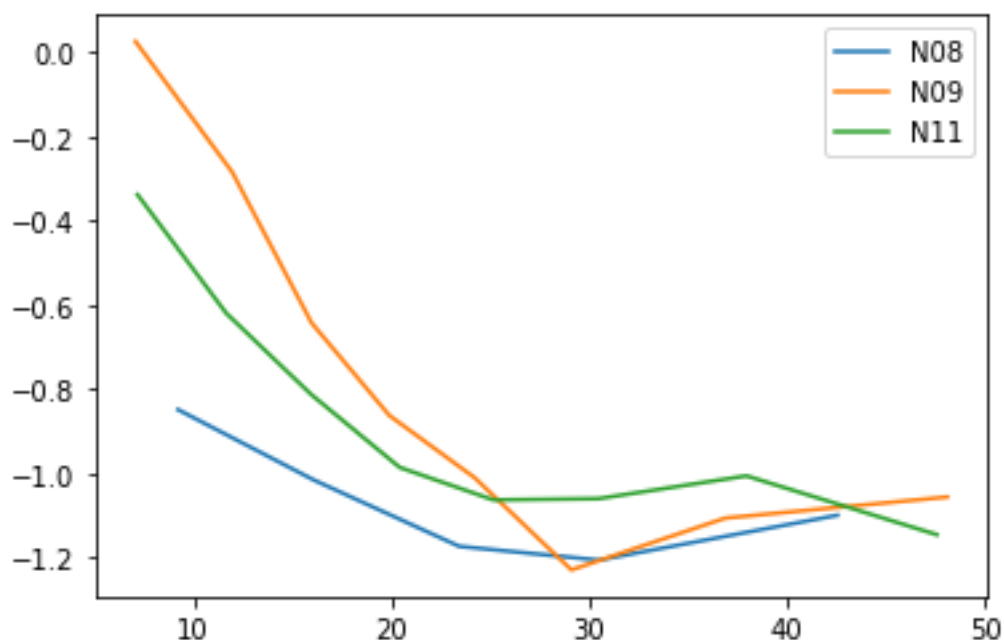

Figure 5. Prior TCWV bias (for clear sky areas) derived from three sensors. Correction in kg m^{-2} versus prior value in kg m^{-2}.

Figure 5 shows the prior TCWV correction for the three platforms. Despite the potential for interaction of calibration, simulation and prior errors in the parameterisation process, the estimates are highly consistent for water vapour loadings in excess of 15 kg m^{-2}, with some divergence for drier atmospheres. Apart from any change in the bias over time, we expect this bias function to be relatively common between sensors, as it is independent of instrument. It is clear that for drier atmospheres there is some variation between the estimates, but it is feasible that the average prior bias correction over these and further sensors to be analysed may provide a better estimate than an individual solution. This will be considered for a future iteration of the process.

4.   CONCLUSION

Algorithm developments in radiative transfer simulation and use in optimal estimation have been presented for improving SSTs for the CDR v3. The analyses shown for the three AVHRRs presented will be extended to all the NOAA platforms and used in L1 to L4 processing. The full set of results will be reflected in the v3 algorithm theoretical basis document that will be prepared for the dataset release, planned for early 2022. The effectiveness of the error covariance matrices in obtaining OE uncertainty estimates will be assessed via validation activities (validation of the uncertainty behaviours).

5. REFERENCES

Block, T., Embacher, S., Merchant, C.J., & Donlon, C. (2018). High-performance software framework for the calculation of satellite-to-satellite data matchups (MMS version 1.2). *Geoscientific Model Development, 11*, 2419-2427

Bozzo, A., Benedetti, A., Flemming, J., Kipling, Z., & Remy, S. (2020). An aerosol climatology for global models based on the tropospheric aerosol scheme in the Integrated Forecasting System of ECMWF. *Geoscientific Model Development, 13*, 1007-1034

Carboni, E., Mather, T.A., Schmidt, A., Grainger, R.G., Pfeffer, M.A., Ialongo, I., & Theys, N. (2019). Satellite-derived sulfur dioxide (SO2) emissions from the 2014-2015 Holuhraun eruption (Iceland). *Atmospheric Chemistry and Physics, 19*, 4851-4862

Cordoba, M., Dance, S.L., Kelly, G.A., Nichols, N.K., & Waller, J.A. (2017). Diagnosing atmospheric motion vector observation errors for an operational high-resolution data assimilation system. *Quarterly Journal of the Royal Meteorological Society, 143*, 333-341

Desroziers, G., Berre, L., Chapnik, B., & Poli, P. (2005). Diagnosis of observation, background and analysis-error statistics in observation space. *Quarterly Journal of the Royal Meteorological Society, 131*, 3385-3396

Hersbach, H., Bell, B., Berrisford, P., Biavati, G., Horányi, A., Muñoz Sabater, J., Nicolas, J., Peubey, C., Radu, R., Rozum, I., Schepers, D., Simmons, A., Soci, C., Dee, D., & Thépaut, J.-N. (2018). ERA5 hourly data on pressure levels from 1979 to present. In. European Centre for Medium-range Weather Forecasting, Reading, UK: Copernicus Climate Change Service (C3S) Climate Data Store (CDS)

Holl, G., Mittaz, J.P.D., & Merchant, C.J. (2019). Error Correlations in High-Resolution Infrared Radiation Sounder (HIRS) Radiances. *Remote Sensing, 11*

Kalman, R.E. (1960). A new approach to linear filtering and prediction problems. *Trans AMSE, Ser. D, J. Basic Eng., 82*

Kilic, L., Prigent, C., Aires, F., Boutin, J., Heygster, G., Tonboe, R.T., Roquet, H., Jimenez, C., & Donlon, C. (2018). Expected Performances of the Copernicus Imaging Microwave Radiometer (CIMR) for an All-Weather and High Spatial Resolution Estimation of Ocean and Sea Ice Parameters. *Journal of Geophysical Research-Oceans, 123*, 7564-7580

Koner, P.K., & Harris, A. (2016). Sea Surface Temperature Retrieval from MODIS Radiances Using Truncated Total Least Squares with Multiple Channels and Parameters. *Remote Sensing, 8*

Koner, P.K., Harris, A., & Maturi, E. (2015). A Physical Deterministic Inverse Method for Operational Satellite Remote Sensing: An Application for Sea Surface Temperature Retrievals. *Ieee Transactions on Geoscience and Remote Sensing, 53*, 5872-5888

McGarragh, G.R., Poulsen, C.A., Thomas, G.E., Povey, A.C., Sus, O., Stapelberg, S., Schlundt, C., Proud, S., Christensen, M.W., Stengel, M., Hollmann, R., & Grainger, R.G. (2018). The Community Cloud retrieval for CLimate (CC4CL) - Part 2: The optimal estimation approach. *Atmospheric Measurement Techniques, 11*, 3397-3431

Merchant, C.J., & Embury, O. (2020). Adjusting for Desert-Dust-Related Biases in a Climate Data Record of Sea Surface Temperature. *Remote Sensing, 12*

Merchant, C.J., Embury , O., Bulgin , C.E., Block, T., Corlett , G.K., Fiedler , E., Good , S.A., Mittaz , J., Rayner , N.A., Berry , D., Eastwood , S., Taylor , M., Tsushima , Y., Waterfall , A., Wilson , R., & Donlon, C. (2019). Satellite-based time-series of sea-surface temperature since 1981 for climate applications. *Scientific Data, in press*

Merchant, C.J., Le Borgne, P., Marsouin, A., & Roquet, H. (2008). Optimal estimation of sea surface temperature from split-window observations. *Remote Sensing of Environment, 112*, 2469-2484

Merchant, C.J., Le Borgne, P., Roquet, H., & Marsouin, A. (2009). Sea surface temperature from a geostationary satellite by optimal estimation. *Remote Sensing of Environment, 113*, 445-457

Merchant, C.J., Saux-Picart, S., & Waller, J. (2020). Bias correction and covariance parameters for optimal estimation by exploiting matched in-situ references. *Remote Sensing of Environment, 237*

Poulsen, C.A., Siddans, R., Thomas, G.E., Sayer, A.M., Grainger, R.G., Campmany, E., Dean, S.M., Arnold, C., & Watts, P.D. (2012). Cloud retrievals from satellite data using optimal estimation: evaluation and application to ATSR. *Atmospheric Measurement Techniques, 5*, 1889-1910

Rodgers, C.D. (2000). *Inverse Methods for Atmospheric Sounding: Theory and Practice*. Singapore: World Scientific Publishing

Saunders, R., Hocking, J., Turner, E., Rayer, P., Rundle, D., Brunel, P., Vidot, J., Roquet, P., Matricardi, M., Geer, A., Bormann, N., & Lupu, C. (2018). An update on the RTTOV fast radiative transfer model (currently at version 12). *Geoscientific Model Development, 11*, 2717-2732

Thomas, G.E., Poulsen, C.A., Sayer, A.M., Marsh, S.H., Dean, S.M., Carboni, E., Siddans, R., Grainger, R.G., & Lawrence, B.N. (2009). The GRAPE aerosol retrieval algorithm. *Atmospheric Measurement Techniques, 2*, 679-701

Waller, J.A., Ballard, S.P., Dance, S.L., Kelly, G., Nichols, N.K., & Simonin, D. (2016). Diagnosing Horizontal and Inter-Channel Observation Error Correlations for SEVIRI Observations Using Observation-Minus-Background and Observation-Minus-Analysis Statistics. *Remote Sensing, 8*